Electrochimica Acta 238 (2017) 81–90

Contents lists available at ScienceDirect

Electrochimica Acta

journal homepage: www.elsevier.com/locate/electacta

Electrochemical generation of a molecular heterojunction. A new Zn-Porphyrin-Fullerene C_{60} Polymeric Film

Claudia Solis[a], M. Belén Ballatore[a], María B. Suarez[a], María Elisa Milanesio[a], Edgardo N. Durantini[a], Marisa Santo[a], Thomas Dittrich[b], Luis Otero[a,*], Miguel Gervaldo[a,*]

[a] Departamento de Química, Universidad Nacional de Río Cuarto, CONICET, Agencia Postal Nro. 3, X5804BYA Río Cuarto, Córdoba, Argentina
[b] Helmholtz Center Berlin for Materials and Energy, Institute of Silicon Photovoltaics, Kekuléstrasse 5, D-12489 Berlin, Germany

ARTICLE INFO

Article history:
Received 7 December 2016
Received in revised form 1 March 2017
Accepted 3 April 2017
Available online 4 April 2017

Keywords:
Porphyrin-fullerene
Surface Photovoltage
Electropolymerization

ABSTRACT

The design and electrosynthesis of electroactive and photoelectroactive polymeric organic thin films holding Zn(II)-porphyrin and Zn(II)-porphyrin-C_{60} dyad are reported. The presence of carbazole substituents in the *meso* positions of the tetrapyrolic macrocycle allows the formation of conducting polymers by coupling of electrogenerated carbazole radical cations. Due to the fact that both donor and acceptor units in the monomer dyad are covalently bonded, a polymeric heterojunction can be formed in just one single step. The ITO/organic polymer electrodes were studied by cyclic voltammetry, UV-visible absorption spectroscopy and spectroelectrochemistry, showing that the porphyrin building blocks were not altered during the polymerization process and that they retained their light harvesting capacity and electrochemical characteristics. Upon illumination of the polymeric films, photoinduced charge separation and charge migration occur. The photovoltage spectra followed very well the absorption spectra of the organic materials, and in ITO/Zn-porphyrin-C_{60} electrodes, the signal amplitude and transitory photovoltage half-life time are larger than those observed for Zn-porphyrin polymer. Thus, a "double cable" polymeric structure is proposed for the material with the presence of the strong electron acceptor C_{60} fullerene, the hole transport porphyrin and dicarbazole moieties, making the material a potential building block for applications in the design and construction of organic optoelectronic devices.

1. Introduction

The development of functional organic materials for their application in organic-based optoelectronic devices is one of the most active research areas, involving the design (often assisted by theoretical computational approach) synthesis, characterization, and practical application in devices construction. Most systems are formed by an electron donor and electron acceptor configuration of chromophores [1], which are able to convert an incident photon into an electrical effect or an electrical pulse into an emitting photon or into color change [2,3]. Charge transport and charge collection (or injection) at organic/metal interfaces are very important issues in the performance of the organic optoelectronic devices, among others aspects. Thus, materials holding tetrapyrrolic ring derivatives (porphyrins and phtalocyanines) have caught high attention in this field [4,5–7]. They are excellent chromophores, with high extinction coefficients, remarkable electron donor-acceptor capabilities and they are able to form p-type semiconducting layers [8,9–11]. Also, these layers can be generated through electrochemical polymerization of adequately substituted tetrapyrrolic compounds [12,13]. Electropolymerization is a very versatile procedure to construct organic layers over metallic contacts, or over transparent conducting oxides [14,15–17] (Indium Tin Oxide, ITO; Fluorine doped Tin Oxide, FTO) that act as translucent windows in the building of optoelectronic devices [14,15–17]. Recently we reported the electrochemical generation of organic-organic heterojunctions, formed by boundaries between electron donor and electron acceptor materials [17,18]. These heterojunctions were built by electropolymerization and film formation of carbazole and/or triphenylamine functionalized porphyrins (metal and free base), and C_{60} buckminsterfullerene. The methodology created electroactive and photoelectroactive films, where photogenerated charge carriers are preferentially separated, as it was demonstrated by surface photovoltage spectroscopy (SPV) studies. Both, spectral and time dependent SPV data showed that the electrons were separated in the direction

* Corresponding authors.
E-mail addresses: lotero@exa.unrc.edu.ar (L. Otero), mgervaldo@exa.unrc.edu.ar, miguel.gervaldo@hotmail.com (M. Gervaldo).

http://dx.doi.org/10.1016/j.electacta.2017.04.015
0013-4686/

of the C_{60} layer, meanwhile the holes were located in the porphyrin internal surface. All these effects showed that the electrochemical generated heterojunctions are efficient in the production of charge separated states, and that could be applied in the development of optoelectronic devices. On the other hand, although there are several reports about the formation of donor-acceptor polymers by electrochemical polymerization of donor-acceptor monomers [19,20–22], there are a couple of examples involving the electropolymerization of porphyrin-C_{60} dyads [23,24]. It is known that porphyrin-C_{60} dyads are very efficient in the formation of photoinduced charge separated states [25,26,27]. Therefore, the use of donor-acceptor monomer dyads could generate polymers where each unit in the material, under illumination, is able to form a charge separated state, acting as a "molecular heterojunction". The modification of these dyads with electropolymerizable groups would permit the generation of polymers by electrochemical methods in just one single step. Gervaldo et al. reported the formation of a photo- and electrochemically-active porphyrin–fullerene dyad electropolymer [23] whose properties showed that light absorption leads to ultrafast (picoseconds) charge separation due to the presence of a molecular heterojunction, which has not requirement of exciton migration. Also, hole mobilities for porphyrin-fullerene electropolymers were evaluated [28] showing that they are larger than those reported for other organic polymers, suggesting that the studied polymers are good candidates for optoelectronic applications.

In the present work, a porphyrin-C_{60} dyad was successfully electropolymerized over Pt and ITO substrates. The monomer (Zn-PCBZ-C_{60}, Fig. 1) was designed and synthetized holding three *N*-ethyl carbazoyl residues that upon oxidation generated carbazole radical cations, which by coupling produced the formation of an extended and branched electroactive conjugated polymer. Also, the use of this new dyad allows the electrosynthesis of a donor-acceptor polymeric heterojunction in just one single step, because the monomer used here presents both, the donor and acceptor units covalently bonded. This polymer formed stable thin films over the electrode surfaces, where the electron acceptor (fullerene) and electron donor (porphyrin) capabilities of the functional groups remained active. This fact was corroborated by UV–vis spectroscopy, electrochemistry, spectroelectrochemistry, and energy and time dependent surface photovoltage studies. Upon porphyrin excitation, photoinduced charge separation and charge migration occurred. The half-life time of the Laser pulse generated transient photovoltage is larger than the same for the homologues porphyrin polymer film, enlighten the effect of the presence of the C_{60} electron acceptor in the polymer structure. These results demonstrate that the material is a promising candidate for application in the development of optoelectronic devices.

2. Experimental section

2.1. Monomer synthesis

Zinc(II) 5,10,15,20-tetrakis[3-(*N*-ethylcarbazoyl)]porphyrin (Zn-PCBZ) was prepared from 5,10,15,20-tetrakis[3-(*N*-ethylcarbazoyl)]porphyrin (TCP) [29]. A solution of TCP (20 mg, 0.018 mmol) in 7 mL of dichloromethane DCM was treated with 2 mL of a saturated solution of zinc(II) acetate in methanol. The mixture was stirred for 1 h in argon atmosphere at room temperature. After that, the reaction mixture was treated with water (30 mL) and the organic phase was extracted with three portions of DCM (10 mL each). The solvents were evaporated under reduced pressure yielding 20 mg (97%) of pure Zn-PCBZ. APPI-MS [m/z] 1145.3998 $[M+H]^+$ (1144.3914 calculated for $C_{76}H_{56}N_8Zn$). Dyad Zn-PCBZ-C_{60} was synthesized from the free-base dyad (20 mg, 0.011 mmol) using the procedure described above for Zn-PCBZ [24]. This approach produced 19 mg (95%) of pure Zn-PCBZ-C_{60}. APPI-MS [m/z] 1803.3841 $[M+H]^+$ (1802.3763 calculated for $C_{131}H_{54}N_8Zn$).

2.2. Instrumentation and measurements

Mass spectra were recorded on a Bruker micrOTOF-QII (Bruker Daltonics, MA, USA) equipped with an atmospheric pressure photoionization (APPI) source. Absorption and fluorescence spectra were recorded using 1 cm path length quartz cells on a Shimadzu UV-2401PC spectrometer and on a Spex FluoroMax fluorometer, respectively. The concentration of monomers in solution used for UV–vis and fluorescence were 1×10^{-6} M and 1×10^{-7} M respectively. The fluorescence quantum yields (Φ_F) of the monomers were calculated by comparison of the area below the corrected emission spectrum in each solvent with that of TCP as a reference. For this purpose, the value of Φ_F for TCP in DCM ($\Phi_F^{DCM} = 0.10$) was calculated by comparison with the fluorescence spectrum in *N,N*-dimethylformamide using $\Phi_F = 0.14$ for TCP and taking into account the refractive index of the solvents [30].

The voltammetric characterization of the redox processes and electropolymerization of the monomers were performed with a potentiostat-galvanostat Autolab (Electrochemical Instruments) using a Pt working electrode and a Pt counter electrode in a conventional three-electrode cell. Indium tin oxide (ITO) electrodes (Delta Technologies) with a nominal resistance of 8–12 Ω/square were also used as working electrodes. When large area ITO

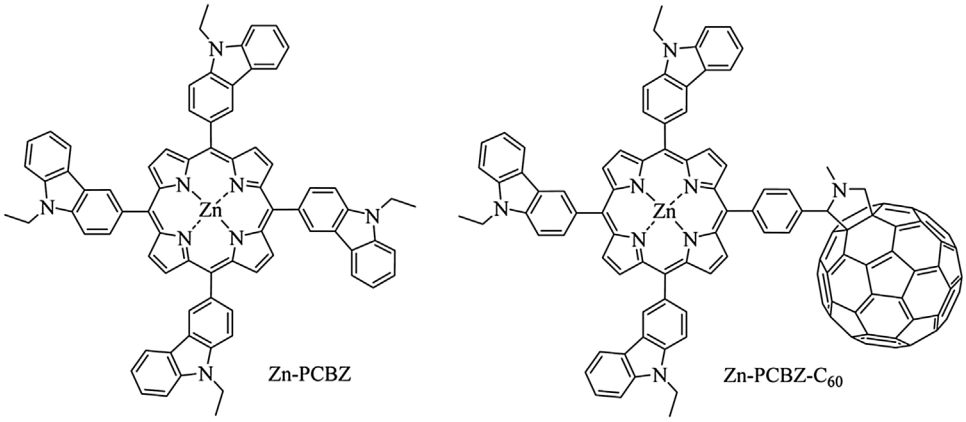

Fig. 1. Chemical structure of Zn-PCBZ and Zn-PCBZ-C_{60}.

electrodes were used, the counter electrode was isolated from the monomer solution by a glass frit in order to avoid interference with the redox reactions occurring at the working electrode. Electrochemical studies of Zn-PCBZ were carried out in 1,2-dichloroethane (DCE) deoxygenated solution (nitrogen bubbling), with 0.10 M tetra-n-butylammonium hexafluorophosphate ($TBAPF_6$) as the supporting electrolyte, and in o-dichlorobenzene (o-DCB) deoxygenated solution (nitrogen bubbling) for Zn-PCBZ-C_{60}, with 0.10 M tetra-n-butylammonium perchlorate as the supporting electrolyte. All the electrochemical responses of the electropolimerized films were carried out in DCE deoxygenated solution (nitrogen bubbling), with 0.10 M $TBAPF_6$. A silver wire quasi-reference electrode was used. The Pt working electrode was cleaned between experiments by polishing with 0.3 μm alumina paste followed by solvent rinses. After each voltammetric experiment, Ferrocene was added as an internal standard, and the potential axis was calibrated against the formal potential for the Saturated Calomel Electrode (SCE).

Spectroelectrochemical experiments were carried out in a homemade cell built from a commercial UV–visible cuvette. The ITO-coated glass was used as working electrode; a Pt wire was used as counter electrode, and an Ag wire was used as the reference electrode. The cell was placed in the optical path of the sample light beam. The background correction was obtained by taking an UV–vis spectrum of a blank cell (an electrochemical cell with an ITO working electrode without the polymer film) with conditions and parameters identical to those of the polymer experiment.

Semiempirical calculations were used to obtain information about molecular geometry and frontier orbital distribution in the studied monomers. Austin Model 1 (AM1, HyperChem package software) with restricted Hartree–Fock basis was employed with the Polak-Ribiere conjugated gradients algorithm. The convergence was set at 0.05 kcal/Å mol.

The measurements of modulated Surface Photovoltage (SPV) were performed in the fixed capacitor arrangement with chopped light (modulation frequency 6 Hz) from a quartz prism monochromator (SPM2) and a halogen lamp (100 W). The modulation period was chosen to be of the same order as the time at which the SPV transients leveled [31]. The measurements were carried out in vacuum using an already described set-up [17,18,32]. SPV transients were excited with laser pulses (wavelength 600 nm, time of laser pulses: 5 ns, intensity: about 3 mJ/cm^2) and recorded with a sampling oscilloscope (GAGE compuscope CS 14200) at resolution of 10 ns. The photoelectrodes were illuminated from the front face (organic polymer surface).

3. Results and discussion

3.1. UV-visible absorption and emission spectroscopy

The absorption spectra of the dyad and the corresponding porphyrin in DCE are shown in Fig. 2a. Both monomers present the typical Soret band and the characteristic *Q*-bands of Zn(II) metalloporphyrins. For the dyad, the absorption in the UV region is stronger than that of the porphyrin due to the presence of the C_{60} moiety, whereas in the visible region the spectrum of the dyad is quite similar to the porphyrin. Zn-PCBZ and Zn-PCBZ-C_{60} present emission bands at similar wavelengths (Fig. 2b), but the fluorescence quantum yield (Φ_F) of the dyad ($(3{,}8 \pm 0{,}3) \times 10^{-3}$) is much lower than that calculated for Zn-PCBZ (0.05 ± 0.01). This very weak emission from the porphyrin moiety in the dyad indicates a strong quenching of the porphyrin excited singlet state by the attached fullerene structure. It has been shown in structurally related porphyrin–C_{60} dyads that the main decay mode of the photoexited porphyrin moiety is a rapid photoinduced intramolecular electron transfer to yield a charge-separated state [25,26,27]. In the present case the energy of Zn-PCBZ$^{+\bullet}$-$C_{60}^{-\bullet}$ state is around 1.22 eV above that of the dyad ground state, which has been estimated from the first oxidation potential of the porphyrin moiety and first reduction potential of C_{60} (obtained by cyclic voltammetry analysis of the dyad, see below). This value lies 0.86 eV below the porphyrin singlet state (2.08 eV), making thermodynamically feasible the quenching of the porphyrin excited singlet state by the attached fullerene structure through charge transfer mechanism [25,26,27].

3.2. Electrochemistry

Cyclic voltammetry was used to characterize the electrochemical properties of Zn-PCBZ and Zn-PCBZ-C_{60}. Fig. 3a shows the first anodic and cathodic scan of Zn-PCBZ, where one reduction peak, and three oxidation processes can be seen. The reduction peak, together with the first two oxidation processes, are assigned to the formation of the radical anion, radical cation, and dication of the porphyrin macrocycle respectively, while the third irreversible wave is attributed to oxidation of the CBZ units [29]. Continuous cycling from −0.40 V to 1.40 V produces an increase in the

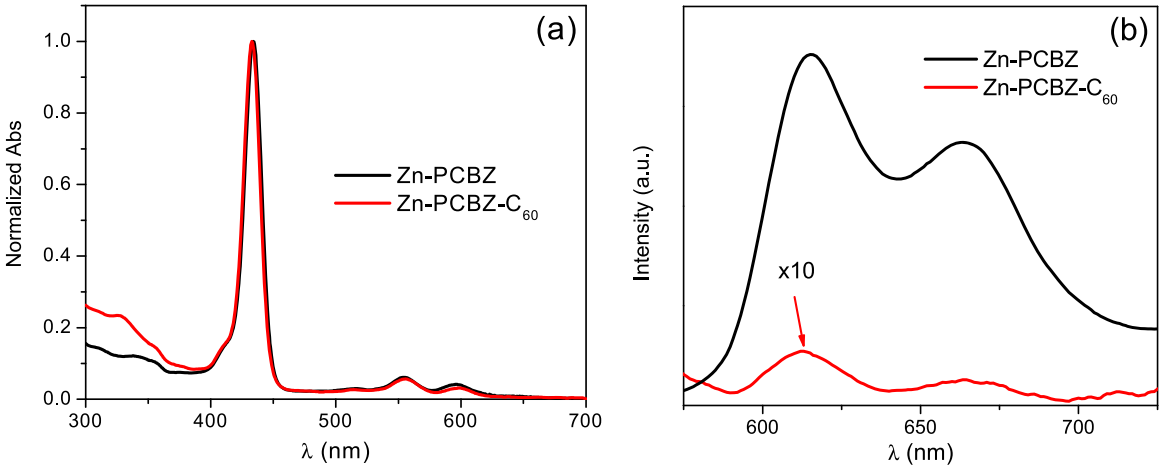

Fig. 2. (a) Absorption spectra and (b) emission spectra of Zn-PCBZ and Zn-PCBZ-C_{60} (x 10) in DCE solution. λ_{exc}: 560 nm.

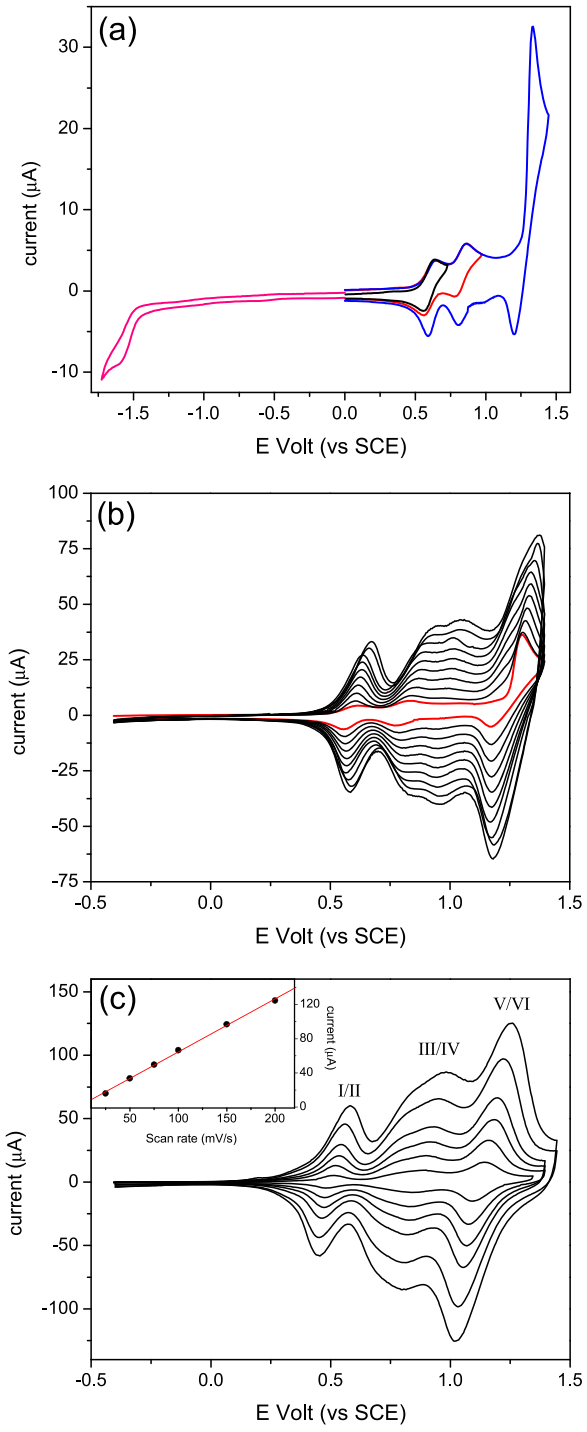

Fig. 3. (a) First anodic and cathodic scans of Zn-PCBZ at different inversion potentials obtained at a scan rate of 100 mV/s. E_i = 0.00 V, Eλ = 0.74 V (black line). E_i = 0.00 V, Eλ = 0.98 V (red line). E_i = 0.00 V, Eλ = 1.45 V (blue line). (b) Ten cyclic voltammogram scans obtained at a scan rate of 100 mV/s. (c) Cyclic voltammograms of a Zn-PCBZ film in solution containing only a support electrolyte. (c-inset) relation between the oxidation peak currents (V) and the scan rate. All the cyclic voltammogram scans were obtained in DCE containing $TBAPF_6$. Pt working electrode. (For interpretation of the references to colour in this figure legend, the reader is referred to the web version of this article.)

oxidation-reduction currents, indicating the formation of a product adsorbed on the electrode surface (Fig. 3b). The electrochemical response of the electrode in a solution containing only support electrolyte, consists of three redox systems which are labeled as I/II, III/IV, and V/VI in Fig. 3c. The first (I/II) and third (V/VI) redox systems present a bell shape, while the second (III/IV) one is a broad peak. A linear relation between the oxidation peak currents and the scan rate is observed for the three redox systems (inset Fig. 3c), confirming the adsorption of a stable and reversible electroactive product on the electrode surface.

On the other hand, Zn-PCBZ-C_{60} presents two reduction processes at around −0.66 and −1.06 V, which are assigned to

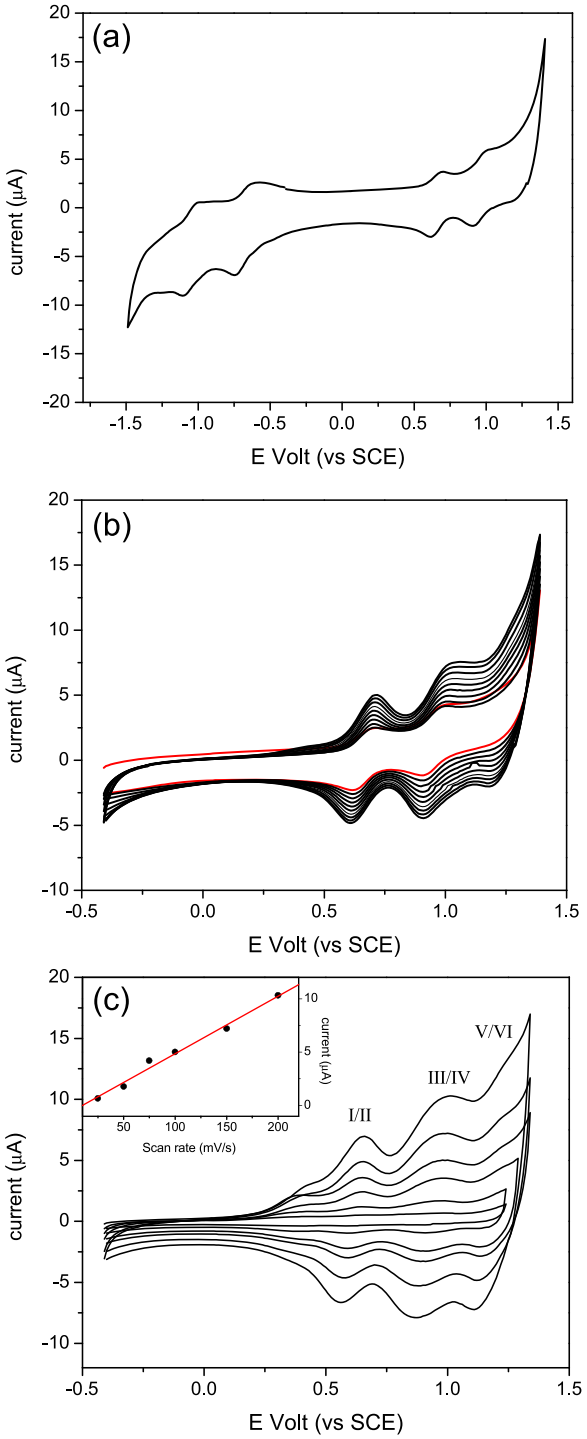

Fig. 4. (a) First anodic and cathodic scans of Zn-PCBZ-C_{60} obtained at a scan rate of 100 mV/s. (b) Ten cyclic successive voltammograms obtained at a scan rate of 100 mV/s. (c) Cyclic voltammograms a Zn-PCBZ-C_{60} film in solution containing only a support electrolyte. (c-inset) Relation between the oxidation peak currents (III) and the scan rate. All the cyclic voltammogram scans were obtained in o-DCB containing TBAP. Pt working electrode.

the formation of the radical anion and dianion of the C_{60} unit, (Fig. 4a) [23]. In the anodic scan two reversible processes can be seen, and they are associated to oxidation of the porphyrin macrocycle. In addition, at more anodic potentials an increase in the oxidation current is observed (which is not present in the blank scan), this could be assigned to oxidation of the CBZ units present in Zn-PCBZ-C_{60}, in concordance with the peak observed in Zn-PCBZ at a similar applied potential. When the electrode is cycled in the anodic range (from −0.40 to 1.40 V) increases in the oxidation/reduction currents can be detected with every new scan (Fig. 4b). The electrochemical response of the electrode (after cycling) in a free Zn-PCBZ-C_{60} solution containing only support electrolyte presents also three redox couples (I/II, III/IV, and V/VI) at similar potentials than those observed in Zn-PCBZ films. The oxidation and reduction peak currents are proportional to the scan rate, typical of an electroactive product adsorbed on the electrode surface (inset Fig. 4c).

Furthermore, AM1 calculations were used to obtain more information about the charge distribution in the different redox processes in Zn-PCBZ-C_{60} monomer. Fig. 5a–b show optimized structures of Zn-PCBZ-C_{60}. The carbazole units and the porphyrin macrocycle plane are spatially twisted one with respect to the other. The HOMO is mainly based on the porphyrin ring π-orbitals, while the LUMO is situated on the C_{60}. Therefore it is possible to assign the first and second oxidation processes observed during the first anodic scan to oxidation of the porphyrin macrocycle, the third one to oxidation of carbazole, and the first reduction peak to the formation of C_{60} radical anion. Moreover, the frontier orbital density calculations are in agreement with the charge transfer mechanism for the porphyrin emission quenching.

Taking into account the electrochemical results and the antecedents for structural related compounds it is possible to propose an electropolimerization mechanism and polymer structure. It has been reported that oxidation of carbazole conducts to dimerization of two radical cations through the coupling in 3,3′ positions, being these dimers more easily oxidized than carbazole monomer [33,34]. Polycarbazole and carbazole based polymers present two oxidation processes, related to formation of cation radical and dication of dicarbazole units [35,36]. It must be remarked that both Zn-PCBZ and Zn-PCBZ-C_{60} have the porphyrin macrocycle linked to *N*-substituted carbazole units with one free position which could be able to form carbazole dimers. Therefore, the generation of Zn-PCBZ and Zn-PCBZ-C_{60} films on the electrode surface, obtained by anodic cycling, could be explained by the coupling of two carbazole radical cations through the 3,3′ free positions, generating dicarbazoles and connecting the monomer units (Fig. 6) [29,34,35].

3.3. Spectroelectrochemistry and proposed polymerization mechanism

The absorption spectrum of Zn-PCBZ film formed by electropolymerization over ITO semitransparent electrodes presents the typical Soret band at around 450 nm, together with the two characteristic *Q* bands of Zn (II) metalloporphyrins (Fig. 7a). Likewise, Zn-PCBZ-C_{60} film shows also the Soret and the two *Q* bands (Fig. 7b). It must be remarked that no absorption bands are observed for both films in the NIR zone, in the reduced state. The similarities between the absorption spectra in solution and those electrodeposited on ITO electrodes confirm that the porphyrin centers have not been altered during the polymerization process.

Spectroelectrochemical studies were carried out in order to obtain more information about the polymerization process of Zn-PCBZ, and Zn-PCBZ-C_{60}. Fig. 8a shows difference absorption spectra (the spectrum obtained at 0 V was subtracted from each individual spectrum and then the resulting spectra were plotted as ΔAbs) of Zn-PCBZ film obtained at different applied potentials. Between −0.40 and 0.40 V the absorption spectra are very similar, they present the Soret and *Q* bands, indicating that the porphyrin macrocycle has not been oxidized in this range. When the applied potential becomes more anodic (0.60 to 0.80 V) the Soret band starts to decrease and two positive bands at around 470 nm and another one between 600 and 850 nm with a maximum at about 700 nm appear. Between 1.00 and 1.20 V a new positive band that extends to IR appears on top of the bands observed between 0.60 and 0.80 V. At more positive applied potentials the band in the IR is decreased and a new more defined band with a maximum at around 670 nm can be seen, indicating the formation of a new oxidized state. Fig. 8b shows the changes in selected traces (440, 470, 700, and 1000 nm) during an anodic scan. As mentioned before, no changes are observed between −0.40 and 0.40 V. At the onset of the first oxidation process of the film (around 0.50 V) the Soret band decreases (black line) and the trace at 470 nm increases in intensity (red line). Also, a small increase in the 700 nm band is observed (blue line), while the decrease in the Soret band is almost constant at 0.80 V. At around 0.80 V (beginning of second oxidation process), the band at 470 nm starts to decrease and at the same time the band at 1000 nm grows in intensity attaining its maximum value at around 1.20 V (pink line). Above 1.20 V the band at 1000 nm is decreased and the band at 700 nm is increased until it reaches the highest value at 1.40 V. The correspondence between the changes in the selected traces and the potentials of the redox processes of the film confirm the existence of three different redox states. In the same way, Fig. 8c shows difference absorption spectra (plotted as ΔAbs) obtained during an anodic scan of Zn-PCBZ-C_{60} film. No changes in the absorption spectra are observed in the −0.40-0.50 V range, showing that the film is not oxidized yet. At more anodic potentials (between 0.60 and 0.80 V)

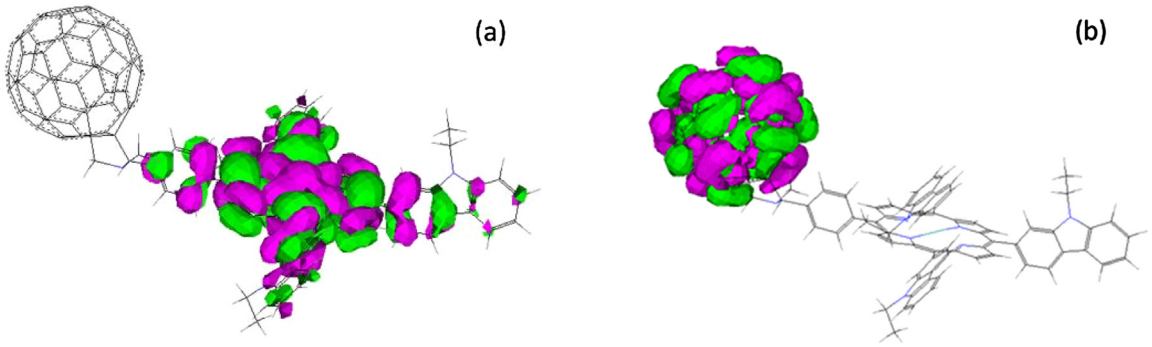

Fig. 5. AM1 optimized structures of Zn-PCBZ-C_{60}. Contour plot of molecular orbitals: (a) HOMO and (b) LUMO.

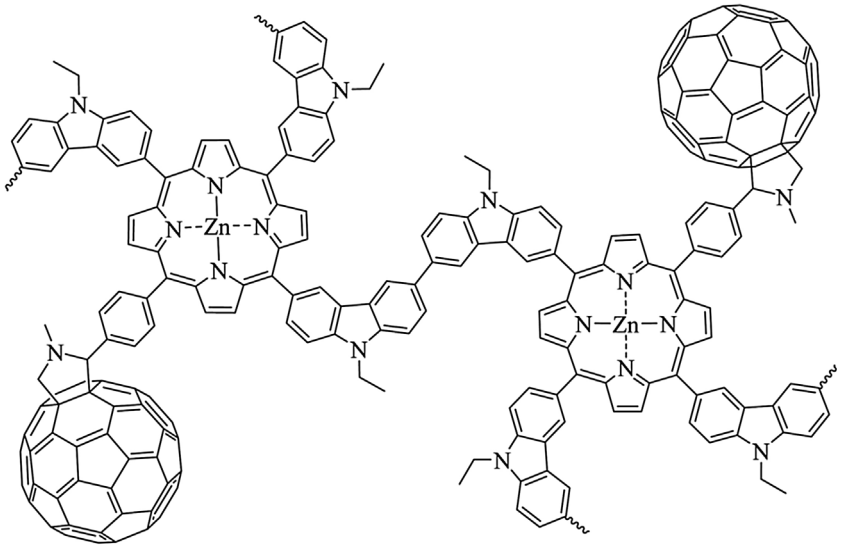

Fig. 6. Proposed structure of Zn-PCBZ-C_{60} polymer.

the Soret band decreases almost completely in intensity and a new positive band at around 700 nm appears. Between 0.80 and 1.20 V a new positive band in the IR zone grows on top of the band detected at 0.60 V. When the film is completely oxidized (1.40 V) a more defined band is observed at around 650 nm.

The electro and spectroelectrochemical data confirm the presence of three redox states in both Zn-PCBZ and Zn-PCBZ-C_{60} films, being these states almost identical in both polymers (see absorption spectra in Fig. 8a and c). The absorption spectra observed in the 0.60 to 0.80 V range are assigned to the radical cation of the porphyrin macrocycle, while the absorption spectra detected between 0.90 and 1.20 V are attributed to formation of the radical cation of the DCBZ units. The absorption spectra obtained at more anodic potentials than 1.20 V are related to the formation of the dication of the DCBZ units. It has been reported that the radical cation of Zn-porphyrins present absorption bands at around 470 and 670 nm. Also in charge separated states of Zn-porphyrin-C_{60} dyads, bands at similar wavelength values have been observed for the radical cation of the porphyrin [37,38]. On the other hand, bands at around 900 and 680 nm have been observed in the first and second oxidation processes of *N*-alkylcarbazoles and poly *N*-alkylcarbazoles, being these bands attributed to the formation of the radical cation and dication of DCBZ units respectively [33,34,35].

The electrochemical and spectroelectrochemical results shown above are in concordance with the presence of DCBZ units in the electropolymeric films of both Zn-PCBZ and Zn-PCBZ-C_{60}. When the monomers are cycled until the furthest oxidation peak, CBZ radical cations are generated and these react to form DCBZ units. The presence of three different redox systems in the polymeric films is related to the formation of porphyrin radical cations, DCBZ radical cations, and DCBZ dications. The absorption spectra obtained in the different redox states are in agreement with the formation of the mentioned oxidized species (porphyrin Soret band bleaching at ~450 nm, DCBZ radical cations at the IR zone and DCBZ dications at ~650 nm). These results are in fully agreement with the polymeric structures exhibited in Fig. 6, where the porphyrin monomers (Zn-PCBZ and Zn-PCBZ-C_{60}) are connected

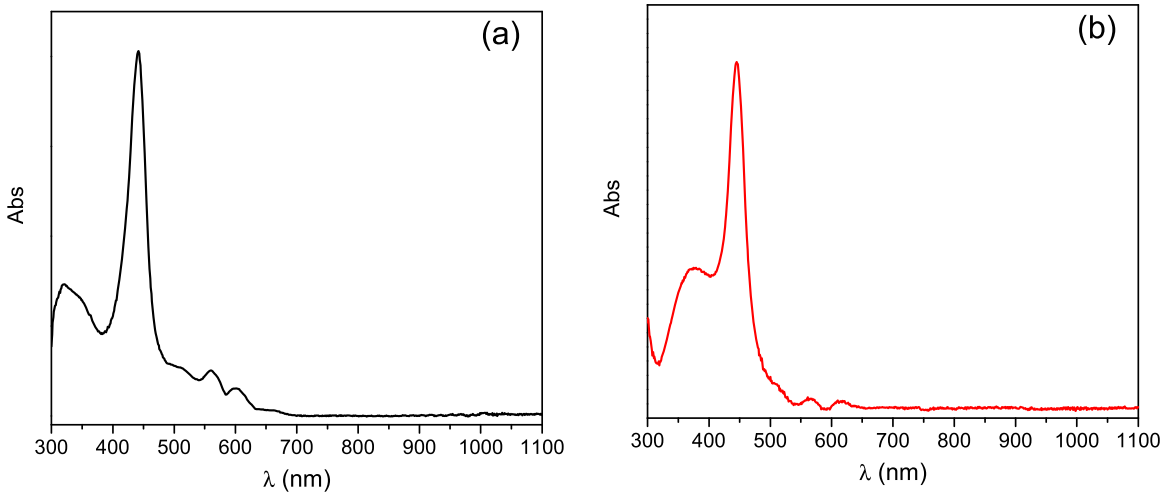

Fig. 7. Absorption spectra of electropolymerized films of (a) Zn-PCBZ and (b) Zn-PCBZ-C_{60} on ITO electrodes.

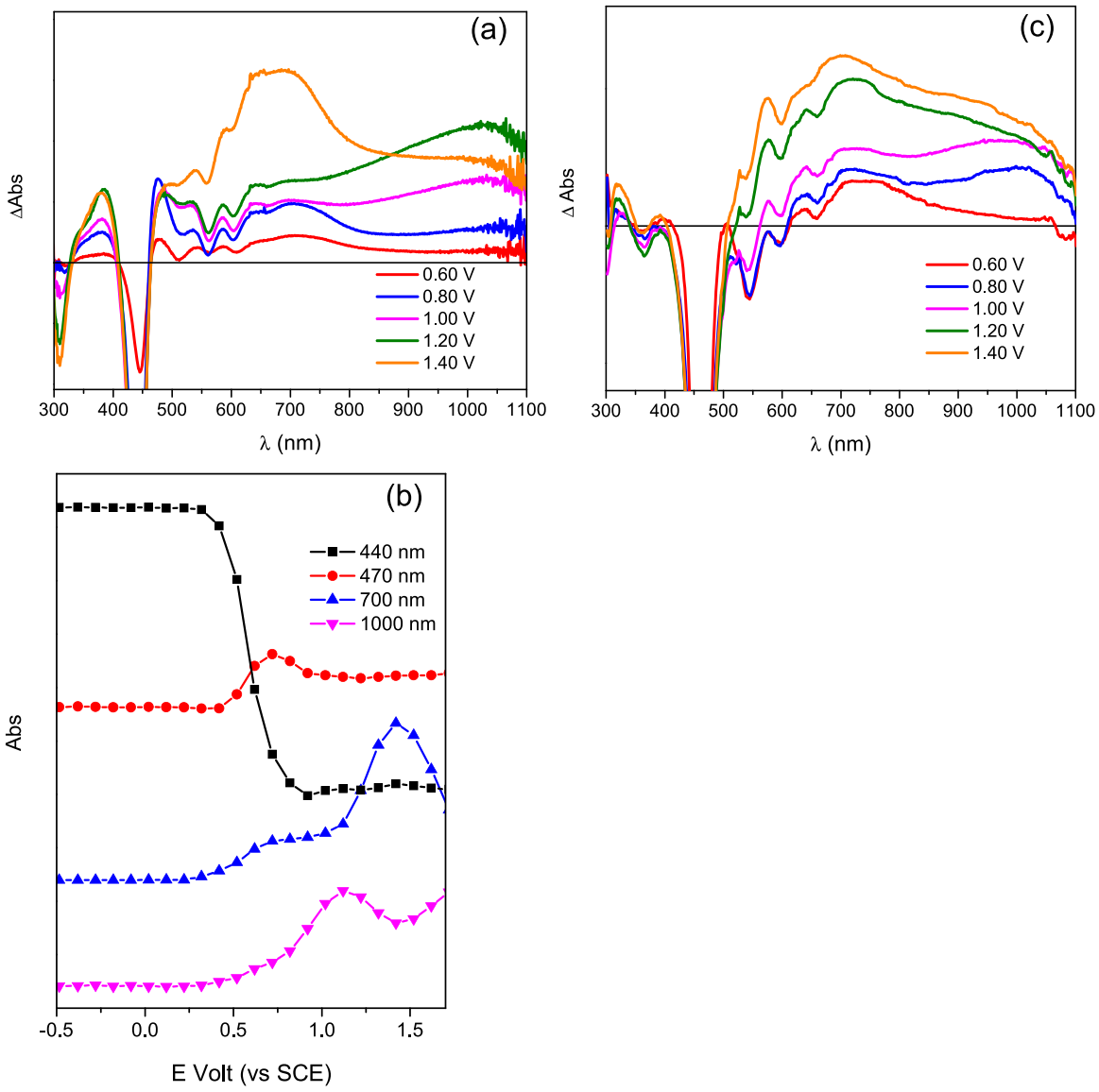

Fig. 8. Spectroelectrochemical measurements of (a) Zn-PCBZ film and, (c) Zn-PCBZ-C_{60} film, at different applied potentials. Absorption traces of (b) Zn-PCBZ film at selected wavelengths as function of the advances in the forward cyclic voltammogram. Scan rate 20 mV/s. For interpretation of the references to colour in the text, the reader is referred to the web version of this article.)

by dicarbazole units. Therefore, a double cable structure for the Zn-PCBZ-C_{60} polymer is proposed, where the porphyrins and dicarbazole units are responsible for the hole transport, while the electrons could be transported by the fullerene units attached to the porphyrin macrocycles [19,20,21].

3.4. Steady state and time resolved surface photovoltage spectroscopy of Zn-PCBZ, and Zn-PCBZ-C_{60} films

Surface photovoltage spectroscopy was used to evaluate the capacity of the films to generate photoinduced charge separated states. Although the ITO/polymer interface affects the SPV generation, as we already reported before [17,18,39], in this new particular case, the presence of C_{60} units in the Zn-PCBZ-C_{60} polymer compared to Zn-PCBZ is analyzed, keeping the ITO/polymer interface nature constant. Fig. 9a–b show the SPV (surface photovoltage) spectra of Zn-PCBZ, and Zn-PCBZ-C_{60} polymer layers, electropolymerized on ITO. In general, the sign of the in-phase SPV signal is negative (positive) if the photogenerated electrons are preferentially separated toward the external (internal) surface. Both, Zn-PCBZ and Zn-PCBZ-C_{60} films present a negative in-phase SPV signal, indicating that the polymers are photoactive and that the electrons are preferentially separated towards the external surface. Moreover, when the photovoltage amplitude spectra are normalized to the photon flux (Fig. 9c–d), they clearly present the typical Soret band and also the two Q bands characteristic of Zn substituted porphyrins, confirming that the light absorption by the organic polymeric film is responsible of the photovoltage generation. It should be noted that the photovoltage amplitude generated for Zn-PCBZ-C_{60} film is around two times larger than the same obtained with Zn-PCBZ polymeric surface (the absorption at Soret band of the samples was similar, ~0.1). On the other hand, evaporated films of C_{60} showed an onset SPV signal at 830 nm with two maxima at 652 and 539 nm [40]. Although these SPV signals occur at similar wavelengths than those observed in Zn-PCBZ-C_{60} and Zn-PCBZ films (Q bands), C_{60} films are not photoactive in the ranges close to the porphyrin Soret band, therefore it is not possible that the increase in SPV signal of Zn-PCBZ-C_{60} compared to Zn-PCBZ is attributed to a contribution of the C_{60} alone. Moreover, C_{60} and PCBM net films form n type

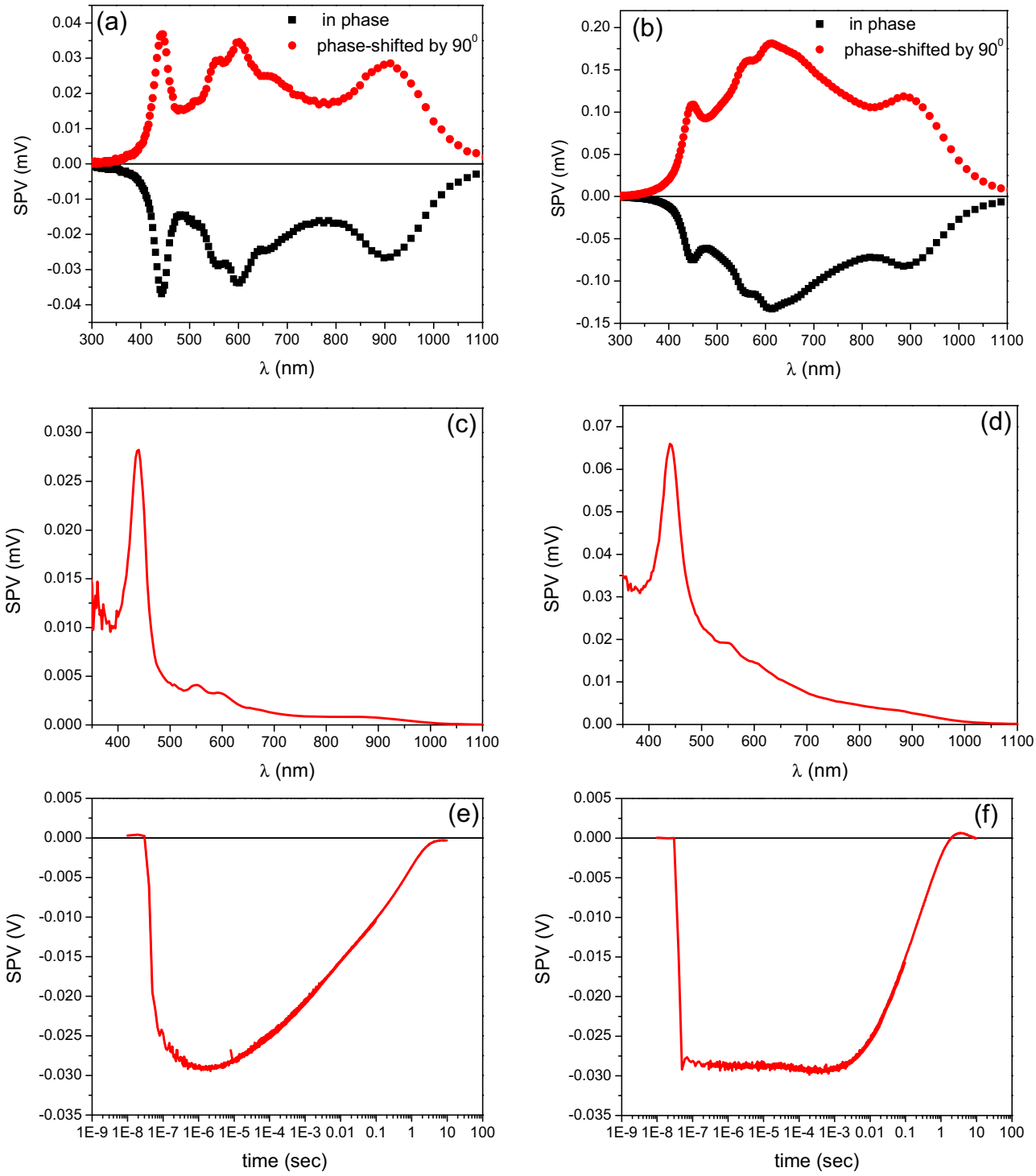

Fig. 9. SPV (surface photovoltage) spectra of electropolymerized films of (a) Zn-PCBZ and (b) Zn-PCBZ-C_{60}. SPV spectra photovoltage amplitude, normalized to the photon flux of (c) Zn-PCBZ and (d) Zn-PCBZ-C_{60} films. Time resolved SPV signals of (e) Zn-PCBZ and (f) Zn-PCBZ-C_{60} films. λ_{exc} = 600 nm.

semiconductors and their morphologic and electronic properties are totally different respect to those attributed to C_{60} in the Zn-PCBZ-C_{60} electropolymerized film, where C_{60} units pendant of the polymeric main chain (as it is shown in Fig. 6). For example, in C_{60} net films there are gap and midgap electronic transitions, which are not possible in the present case [40,41].

Time resolved surface photovoltage measurements were also used to study the generation and recombination kinetics of the photoinduced charge separation states. The sign of the SPV signal for both electropolymers is negative, in concordance with the data obtained under chopped light. As it can observed in Fig. 9e–f, although the magnitude of the SPV signal is similar for Zn-PCBZ and Zn-PCBZ-C_{60} films, the SPV signal for Zn-PCBZ increased very fast after laser pulse from 0 to around 25 mV, then kept growing until 30 mV (between 7×10^{-8} and 2×10^{-6} sec), and then it decreased. For Zn-PCBZ-C_{60} the SPV signal increased faster compared with Zn-PCBZ to around 30 mV, and it remained almost constant. The half-life time of the Laser induced photovoltage in Zn-PCBZ-C_{60} (~0.10 sec) is near one order of magnitude larger than the same for Zn-PCBZ, making evident the effect of the presence of

the strong electron acceptor C_{60} fullerene in the polymer structure. It has been demonstrated that a C_{60} layer evaporated onto MoO3 showed an SPV transitory signal which was characterized by a fast increase within the resolution time of the system, and after the increase, the signal decreased in time continuously [42]. Therefore, it is not possible that the long half-life time observed in Zn-PCBZ-C_{60} compared to Zn-PCBZ is attributed to a contribution of the C_{60} alone. The fast increase in the SPV signal of Zn-PCBZ-C_{60} compared with Zn-PCBZ, could be attributed to a fast generation of charge separated states after light absorption, and to the close proximity between the donor and acceptor parts of the dyad in the polymer structure. It has been demonstrated in structural related porphyrin-C_{60} dyad polymers [23,24], and porphyrin-C_{60} monomer dyads [26,27] that the main decay pathway after light absorption is a ultrafast (ps) photoinduced electron transfer from the porphyrin to the C_{60} to form the $P^{+\bullet}$-$C_{60}^{-\bullet}$ state. This step in the charge separation mechanism is not possible in porphyrin/C_{60} bilayers [18], where the charges must reach the film boundaries, before separation. Consequently, the slow increase in the SPV signal in time of Zn-PCBZ film is attributed to a continuous charge separation by diffusion of photo-generated charge carriers [18,39].

4. Conclusions

Polymeric thin films holding Zn-porphyrin and Zn-porphyrin-C_{60} dyad were successfully formed by electrochemical polymerization over Pt and ITO electrodes. The dyes were designed and synthesized so that the coupling of the electrogenerated carbazole radical cations allowed the polymer formation. The electrochemical formation of the photo and electroactive films was corroborated by cyclic voltammetry, UV-visible absorption spectroscopy and spectroelectrochemical analysis. The studies also confirm that the dyes were not altered during the polymerization process and retained their light harvesting capacity and electrochemical characteristics. Upon illumination both, ITO/Zn-porphyrin and ITO/Zn-porphyrin-C_{60} electrodes, generated surface photovoltages, where the electrons preferably diffused to the external surface meanwhile the holes traveled to the ITO/polymer interface. The PV spectra fully matched the absorption spectra of the polymeric materials, and in ITO/Zn-porphyrin-C_{60} electrodes, the signal amplitude at the Soret band was around two times higher than the same observed for ITO/Zn-porphyrin photoelectrodes. Also, the laser induced transit photovoltage half-life time in ITO/Zn-porphyrin-C_{60} was one order of magnitude larger than the same detected for Zn-porphyrin polymer. Due to the presence of the strong electron acceptor C_{60} fullerene in the polymer and the hole transport capacity of porphyrin and dicarbazole moieties, a “double cable” polymeric structure is suggested for the synthesized material, that is able to produce photoinduced charge separated states with potential applications in the design and construction of organic optoelectronic devices.

Acknowledgments

Authors are grateful to Secretaría de Ciencia y Técnica, Universidad Nacional de Río Cuarto (Secyt-UNRC), Consejo Nacional de Investigaciones Científicas y Técnicas (CONICET)and Agencia Nacional de Promoción Científica y Tecnológica (ANPCYT) of Argentina for financial support. L.O., M.E.M., E.N.D., and M.G., are Scientific Members of CONICET. C.S, M.B.B, and M.B.S thank to CONICET, for research fellowships.

References

[1] T.D. Kim, K.S. Lee, D-π-A Conjugated Molecules for Optoelectronic Applications, Macromol. Rapid Commun. 36 (2015) 943–958.
[2] H. Benten, D. Mori, H. Ohkita, S. Ito, Recent Research Progress of Polymer Donor/Polymer Acceptor Blend Solar Cells, J. Mater. Chem. A 4 (2016) 5340–5365.
[3] S.Y. Lee, T. Yasuda, H. Komiyama, J. Lee, C. Adachi, Thermally Activated Delayed Fluorescence Polymers for Efficient Solution-Processed Organic Light-Emitting Diodes, Adv. Mater. 28 (2016) 4019–4024.
[4] L.-L. Li, E.W.-G. Diau, Porphyrin-Sensitized Solar Cells, Chem. Soc. Rev. 42 (2013) 291–304.
[5] T. Higashino, H. Imahori, Porphyrins as Excellent Dyes for Dye-Sensitized Solar Cells: Recent Developments and Insights, Dalton Trans. 44 (2015) 448–463.
[6] M. Urbani, M. Grätzel, M.K. Nazeeruddin, T. Torres, Meso-Substituted Porphyrins for Dye-Sensitized Solar Cells, Chem. Rev. 114 (2014) 12330–12396.
[7] H. Imahori, T. Umeyama, K. Kurotobi, Y. Takano, Self-Assembling Porphyrins and Phthalocyanines for Photoinduced Charge Separation and Charge Transport, Chem. Commun. 48 (2012) 4032–4045.
[8] J.M. Gottfried, Surface Chemistry of Porphyrins And Phthalocyanines, Surf. Sci. Rep. 70 (2015) 259–379.
[9] D.M. Lyons, J. Kesters, W. Maes, C.W. Bielawski, J.L. Sessler, Improving Efficiencies by Modulating the Central Metal Ion in Porphyrin-Oligothiophene-Mediated P3HT/PCBM Organic Solar Cells, Synth. Met. 178 (2013) 56–61.
[10] H. Qin, L. Li, F. Guo, S. Su, J. Peng, Y. Cao, X. Peng, Solution-Processed Bulk Heterojunction Solar Cells Based on a Porphyrin Small Molecule with 7% Power Conversion Efficiency, Energy Environ. Sci. 7 (2014) 1397–1401.
[11] J. Kesters, P. Verstappen, M. Kelchtermans, L. Lutsen, D. Vanderzande, W. Maes, Porphyrin-Based Bulk Heterojunction Organic Photovoltaics: The Rise of the Colors of Life, Adv. Energy Mater. 5 (2015) 1500218-n/a.
[12] M. Gervaldo, M. Funes, J. Durantini, L. Fernandez, F. Fungo, L. Otero, Electrochemical Polymerization of Palladium (II) and Free Base 5,10,15,20-tetrakis(4-N,N-diphenylaminophenyl)Porphyrins: Its Applications as Electrochromic and Photoelectric Materials, Electrochim. Acta 55 (2010) 1948–1957.
[13] P.A. Liddell, M. Gervaldo, J.W. Bridgewater, A.E. Keirstead, S. Lin, T.A. Moore, A.L. Moore, D. Gust, Porphyrin-Based Hole Conducting Electropolymer, Chem. Mater. 20 (2008) 135–142.
[14] B. Lu, J. Yan, J. Xu, S. Zhou, X. Hu, Novel Electroactive Proton-Doped Conducting Poly(aromatic ethers) with Good Fluorescence Properties via Electropolymerization, Macromolecules 43 (2010) 4599–4608.
[15] L. Xu, J. Zhao, C. Cui, R. Liu, J. Liu, H. Wang, Electrosynthesis and Characterization of an Electrochromic Material from poly(1,4-bis(2-thienyl)-benzene) and its Application in Electrochromic Devices, Electrochim. Acta 56 (2011) 2815–2822.
[16] M. Li, S. Tang, F. Shen, M. Liu, F. Li, P. Lu, D. Lu, M. Hanif, Y. Ma, The Counter Anionic Size Effects on Electrochemical, Morphological, and Luminescence Properties of Electrochemically Deposited Luminescent Films, J. Electrochem. Soc. 155 (2008) H287–H291.
[17] M.B. Suarez, J. Durantini, L. Otero, T. Dittrich, M. Santo, M.E. Milanesio, E. Durantini, M. Gervaldo, Electrochemical Generation of Porphyrin-Porphyrin and Porphyrin-C_{60} Polymeric Photoactive Organic Heterojunctions, Electrochim. Acta 133 (2014) 399–406.
[18] J. Durantini, M.B. Suarez, M. Santo, E. Durantini, Th. Dittrich, L. Otero, M. Gervaldo, Photoinduced Charge Separation in Organic-Organic Heterojunctions Based on Porphyrin Electropolymers. Spectral and Time Dependent Surface Photovoltage Study, J. Phys. Chem. C 119 (2015) 4044–4051.
[19] P. Piotrowski, K. Zarebska, M. Skompska, A. Kaim, Electrodeposition and Properties of Donor-Acceptor Double-Cable Polythiophene with High Content of Pendant Fulleropyrrolidine Moieties, Electrochim. Acta 148 (2014) 145–152.
[20] F.B. Koyuncua, S. Koyuncub, Eyup Ozdemir, A New Donor–Acceptor Carbazole Derivative: Electrochemical Polymerization and Photo-Induced Charge Transfer Properties, Synth. Met. 161 (2011) 1005–1013.
[21] N. Berton, I. Fabre-Francke, D. Bourrat, F. Chandezon, S. Sadki, Poly (bisthiophene-carbazole-fullerene) Double-Cable Polymer as New Donor-acceptor Material: Preparation and Electrochemical and Spectroscopic Characterization, J. Phys. Chem. B 113 (2009) 14087–14093.
[22] T.X. Lava, F. Tran-Van, P.H. Aubert, C. Chevrot, Elaboration and Characterization of Donor–Acceptor Polymer Through Electropolymerization of Fullerene Substituted N-Alkylcarbazole, Synth. Met. 162 (2012) 1923–1929.
[23] M. Gervaldo, P.A. Liddell, G. Kodis, B.J. Brennan, C.R. Johnson, J.W. Bridgewater, A.L. Moore, T.A. Moore, D. Gust, A Photo- and Electrochemically-Active Porphyrin-Fullerene Dyad Electropolymer, Photochem. Photobiol. Sci. 9 (2010) 890–900.
[24] M.B. Ballatore, M.B. Spesia, M.E. Milanesio, E.N. Durantini, Synthesis, Spectroscopic Properties and Photodynamic Activity Of Porphyrin–Fullerene C_{60} Dyads with Application in the Photodynamic Inactivation of Staphylococcus Aureus, Eur. J. Med. Chem. 83 (2014) 685–694.
[25] M.E. Milanesio, M. Gervaldo, L.A. Otero, L. Sereno, J.J. Silber, E.N. Durantini, Synthesis and Photophysical Properties of Zn(II) Porphyrin–C_{60} Dyad with Potential Use in Solar Cells, J. Phys. Org. Chem. 15 (2002) 844–851.
[26] F. D'Souza, S. Gadde, D.M.S. Islam, C.A. Wijesinghe, A.L. Schumacher, M.E. Zandler, Y. Araki, O. Ito, Multi-Triphenylamine-Substituted Porphyrin-Fullerene Conjugates as Charge Stabilizing Antenna-Reaction Center Mimics, J. Phys. Chem. A 111 (2007) 8552–8560.
[27] A.S. Konev, A.F. Khlebnikov, P.I. Prolubnikov, A.S. Mereshchenko, A.V. Povolotskiy, O.V. Levin, A. Hirsch, Synthesis of New Porphyrin–Fullerene Dyads Capable of Forming Charge-Separated States on a Microsecond Lifetime Scale, Chem. Eur. J. 21 (2015) 1237–1250.

[28] B.J. Brennan, P.A. Liddell, T.A. Moore, A.L. Moore, D. Gust, Hole Mobility in Porphyrin- and Porphyrin-Fullerene Electropolymers, J. Phys. Chem. B 117 (2013) 426–432.
[29] J. Durantini, L. Otero, M. Funes, E.N. Durantini, F. Fungo, M. Gervaldo, Electrochemical Oxidation-Induced Polymerization of 5,10,15,20-tetrakis[3-(N-ethylcarbazoyl)]Porphyrin. Formation and Characterization of a Novel Electroactive Porphyrin Thin Film, Electrochim. Acta 56 (2011) 4126–4134.
[30] D.D. Ferreyra, M.B. Spesia, M.E. Milanesio, E.N. Durantini, Synthesis and Photodynamic Properties of 5, 10, 15, 20-tetrakis [3-(N-ethyl-N-methylcarbazoyl)] Chlorin and its Analogous Porphyrin in Solution and in Human Red Blood Cells, J. Photochem. Photobiol. A 282 (2014) 16–24.
[31] Y. Zidon, Y. Shapira, Th. Dittrich, Modulated Charge Separation at Tetraphenyl Porphyrin/Au Interfaces, Appl. Phys. Lett. 90 (2007) 142103-3.
[32] T. Dittrich, S. Bönisch, P. Zabel, S. Dube, High Precision Differential Measurement of Surface Photovoltage Transients on Ultrathin Cds Layers, Rev. Sci. Instrum. 79 (2008) 113903.
[33] J.F. Ambrose, R.F. Nelson, Anodic Oxidation Pathways of Carbazoles: I. Carbazole and N-Substituted Derivatives, J. Electrochem. Soc. 115 (1968) 1159–1164.
[34] J.F. Ambrose, L.L. Carpenter, R.F. Nelson, Electrochemical and Spectroscopic Properties of Cation Radicals: III. Reaction Pathways of Carbazolium Radical Ions, J. Electrochem. Soc. 122 (1975) 876–894.
[35] G.A. Sotzing, J.L. Reddinger, A.R. Katritzky, J. Soloducho, R. Musgrave, J.R. Reynolds, P.J. Steel, Multiply Colored Electrochromic Carbazole-Based Polymers, Chem. Mater. 9 (1997) 1578–1587.
[36] J. Natera, L. Otero, F. D'Eramo, L. Sereno, F. Fungo, N.-S. Wang, Y.-M. Tsai, K.-T. Wong, Synthesis and Properties of a Novel Cross-Linked Electroactive Polymer Formed from a Bipolar Starburst Monomer, Macromolecules 42 (2009) 626–635.
[37] M.E. El-Khouly, K.-J. Han, K.-Y. Kay, S. Fukuzumi, Stabilization of the Charge-Separated States of Covalently Linked Zinc Porphyrin–Triphenylamine–[60] Fullerene, ChemPhysChem 11 (2010) 1726–1734.
[38] D.M. Guldi, Fullerene-Porphyrin Architectures; Photosynthetic Antenna and Reaction Center Models, Chem. Soc. Rev. 31 (2002) 22–36.
[39] J. Durantini, G.M. Morales, M. Santo, M. Funes, E.N. Durantini, F. Fungo, T. Dittrich, L. Otero, M. Gervaldo, Synthesis and Characterization of Porphyrin Electrochromic and Photovoltaic Electropolymers, Org. Electron. 13 (2012) 604–614.
[40] N. Morzé, Th. Dittrich, W. Calvet, I. Lauermann, M. Rusu, Transient and Modulated Charge Separation at $CuInSe_2/C_{60}$ and $CuInSe_2$/ZnPc Hybrid Interfaces, Applied Surface Science 396 (2017) 366–374.
[41] F.E. Osterloh, M.A. Holmes, J. Zhao, L. Chang, S. Kawula, J.D. Roehling, A.J. Moule, P3HT:PCBM Bulk-Heterojunctions: Observing Interfacial and Charge Transfer States with Surface Photovoltage Spectroscopy, J. Phys. Chem. C 118 (2014) 14723–14731.
[42] S. Fengler, Th. Dittrich, M. Rusu, Electronic transitions and Band Offsets in C_{60}: SubPc and C_{60}:MgPc on MoO_3 Studied by Modulated Surface Photovoltage Spectroscopy, J. Appl. Phys. 118 (2015) 035501-1-7.